Hindawi Publishing Corporation
Journal of Nanomaterials
Volume 2016, Article ID 9705257, 9 pages
http://dx.doi.org/10.1155/2016/9705257

Research Article

Woven Glass Fiber Composites with Aligned Carbon Nanotube Sheet Interlayers

Hardik Bhanushali and Philip D. Bradford

Department of Textile Engineering Chemistry and Science, North Carolina State University, Raleigh, NC 27695, USA

Correspondence should be addressed to Philip D. Bradford; philip_bradford@ncsu.edu

Received 14 September 2015; Accepted 23 November 2015

Academic Editor: Hassan Karimi-Maleh

This investigation describes the design, fabrication, and testing of woven glass fiber reinforced epoxy matrix laminates with aligned CNT sheets integrated between plies in order to improve the matrix dominated through thickness properties such as the interlaminar fracture toughness at ply interfaces. Using aligned CNT sheets allows for a concentration of millimeter long CNTs at the most likely point of laminate failure. Mode I and Mode II interlaminar fracture toughness of various CNT modified samples were investigated using double cantilever beam (DCB) and end notched flexure (ENF) experiments, respectively. Short beam strength (SBS) and in-plane tensile properties of the CNT modified samples were also investigated. Moderate improvement was observed in Mode I and Mode II fracture toughness at crack initiation when aligned CNT sheets with a basis weight of 0.354 g/m^2 were used to modify the ply interface. No compromise in the in-plane mechanical properties of the laminate was observed and very little improvement was observed in the shear related short beam strength of the CNT modified laminates as compared to the control samples. Integration of aligned CNT sheets into the composite laminate imparted in-plane and through thickness electrical properties into the nonconductive glass fiber reinforced epoxy composite laminates.

1. Introduction

Fiber reinforced composites have seen an increasing presence in automotive, aerospace, and marine industry due to their high specific strength, stiffness, low density, and high durability [1–3]. These features are achieved due to the excellent fiber dominated in-plane properties of composites which can be tailored according to the design requirements for many specialized applications. Unlike their in-plane properties, the through thickness properties of composites, such as delamination resistance, are generally less than desired. These through thickness properties are controlled by the matrix dominated interlaminar region and the relatively weak fiber-matrix interface [4] whose properties are lower than the reinforcing fiber by an order of 10–20x. This makes the composites susceptible to out of plane damage which can occur through matrix cracking and interfacial failure leading to delamination. Delamination, which is known as a life-limiting damage, severely reduces the overall in-plane compressive properties which render the composite unfit for load bearing structural applications [5, 6]. Interlaminar fracture toughness and interfacial shear strength between the fiber and matrix are the important parameters that determine the through thickness properties of the composites. Mechanical solutions such as stitching [7] and z-pinning [8], changing the fiber architecture by braiding [9] and 3D weaving [10], toughening the resins by incorporating toughening agents [11] or thermoplastic binders, and interleaving [12–14] have been developed to improve interlaminar fracture toughness. However most of these developments result in compromising the in-plane mechanical properties; where stitching, braiding, 3D weaving, and z-pinning reduce the overall in-plane properties, toughened resins and interleaving can degrade the compressive strength of the composite if not incorporated thoughtfully. Micro- and nanosized fillers are also used to improve interlaminar properties [15–17]. A limitation of these additives is the formation of large stress concentrations around agglomerated fillers. Extensive research has been

conducted where nanoparticle fillers, such as carbon nanotubes (CNTs), are incorporated into resins with the purpose of achieving superior through thickness properties without compromising the in-plane properties. CNTs have proven themselves effective in improving the matrix properties and in facilitating load transfer from the matrix to the fiber, thus improving the fiber-matrix interface resulting in improved delamination resistance [18–22].

Owing to their small size, light-weight, extraordinary mechanical, electrical, and thermal properties along with their large aspect ratio and higher specific surface area [1], CNTs have been used in various forms to impart multifunctionality to composite materials [23–26]. CNTs can be used as effective reinforcements and sensors simultaneously due to their exceptional strength, stiffness, and failure strain along with their characteristic electrical response to the applied load [27–30]. CNTs have also been used to improve the thermal, electrical, and mechanical properties of the resins as compared to the base polymer [31–36]. However, the CNTs properties are often not utilized to their fullest due to their tendency to agglomerate within the polymer. Dispersing techniques like direct mixing, mechanical stirring, sonication, and high shear mixing are therefore used to break the agglomerates and achieve uniform dispersion [37, 38]. Improvements in through thickness properties have also been achieved by directly growing the CNTs on the reinforced fiber [23, 39]. Even though it has proven to be an effective method for improving the through thickness properties, this process has a limitation on the type and the size of the reinforcement used.

This investigation is focused on processing composite laminates by incorporating CNTs into the interlaminar region using a novel method of drawing aligned CNT sheets onto prepreg fabrics before lamination and consolidation. This is the first reported use of CNT sheets in this way. The CNTs in the sheets have a very high aspect ratio of ~ 50,000 and are relatively unbundled which allows for uniform resin penetration throughout the CNT interlayer. Uniform CNT placement throughout the laminate was achieved with active control over CNT location and 2D orientation. This processing technique allows for an overall low weight fraction of CNTs to be utilized in the composite; however the CNTs are concentrated where they are needed the most, at the interface between fabric layers. Ideally, this should allow for a higher fracture toughness increase per unit weight of CNTs than in previous studies.

2. Material and Methods

2.1. Materials. Eight harness satin weave E-glass fabric prepregs (Fibre Glast Developments Corp) were used. The areal weight and ply thickness of the individual prepreg fabric used were 298 g/m^2 and 0.22 mm. The nominal resin content was in the range from 27.0% to 33.0% as specified by the manufacturer. The drawable CNT arrays used in this investigation were synthesized in house using the low pressure chemical vapor deposition route based on the method described in [40] and detailed in previous work [41]. The arrays used in this work were approximately 100 × 50 × 1.5 mm. Continuous, 50 mm wide, aligned CNT sheets were easily drawn out horizontally from the vertically aligned CNT arrays (Figure 1(a)).

2.2. Laminate Fabrication. The aligned CNT sheet was then transferred onto the entire length of the prepreg ply (Figure 1(b)) in either parallel or perpendicular direction to the fabric warp direction during ply layup. Owing to the ply's tackiness, the CNT sheet easily adhered to the ply. Each ply was oriented with the technical back of fabric layer facing the midplane to achieve a symmetric laminate [42]. A 60 mm wide, 13 μm thick film of Teflon was laid at the midplane to form an initial crack in the specimens used to test the interlaminar fracture properties. The layup was then consolidated and cured using vacuum bagging and high pressure hot press. A steel plate was used as a one-sided tool to achieve flat specimens. The layup was placed between two nylon peel-ply sheets. This assembly was then covered by high fill nonwoven polyester fabric which was used as a bleeder cloth. The whole assembly was then sealed and vacuum was applied (Figure 1(d)). The specimens were then cured in the hot press for 1 hour at a temperature of 154°C and pressure of 0.38 MPa.

Five different types of specimens were prepared: baseline (no CNTs), 2-layer parallel (basis weight of CNT fabric of 0.354 g/m^2), 2-layer perpendicular (basis weight of CNT fabric of 0.354 g/m^2), 4-layer perpendicular (basis weight of CNT fabric of 0.708 g/m^2), and 8-Layer perpendicular (basis weight of CNT fabric of 1.41 g/m^2). The number refers to the layers of aligned CNT sheets laid in the ply interface and the "parallel" and "perpendicular" refers to the direction of CNT sheet alignment with respect to the warp direction of the woven fabric. Using the basis weight of individual CNT sheets and the mass of the composite panels it was estimated that the weight fraction of CNTs in the composites, with two layers of CNTs added in between every fabric layer, was 0.1%.

2.3. Mechanical and Physical Testing. The DCB test and ENF test data reduction followed ASTM D5528 [43] and JIS K 7086 [44] for determining the Mode I and II interlaminar fracture toughness of both baseline samples and those modified with CNT sheet interlayers. A 24-ply symmetric laminate was stacked and consolidated to achieve a laminate thickness on the order of 4 mm–5 mm where the midplane and two adjoining plies were modified with aligned CNT sheets. Specimens of similar dimensions were fabricated for both the above-mentioned tests. The length L of the specimens was in the range of 150–160 mm. The width B and the thickness, 2 h, of the specimens used were in the range of 24–26 mm and 4.3–4.6 mm, respectively. The initial crack length a_o, created by the Teflon layer, was in the range of 25–32 mm. DCB specimens were coated with white spray on one side followed by marking it with a suitable scale for easy detection of crack growth. Steel piano hinges were used in this investigation to apply Mode I displacement to the specimens. The test was carried out at a constant crosshead speed of 2 mm/min using MTS Q-test tensile testing frame. Crack propagation was manually observed using a magnifying glass.

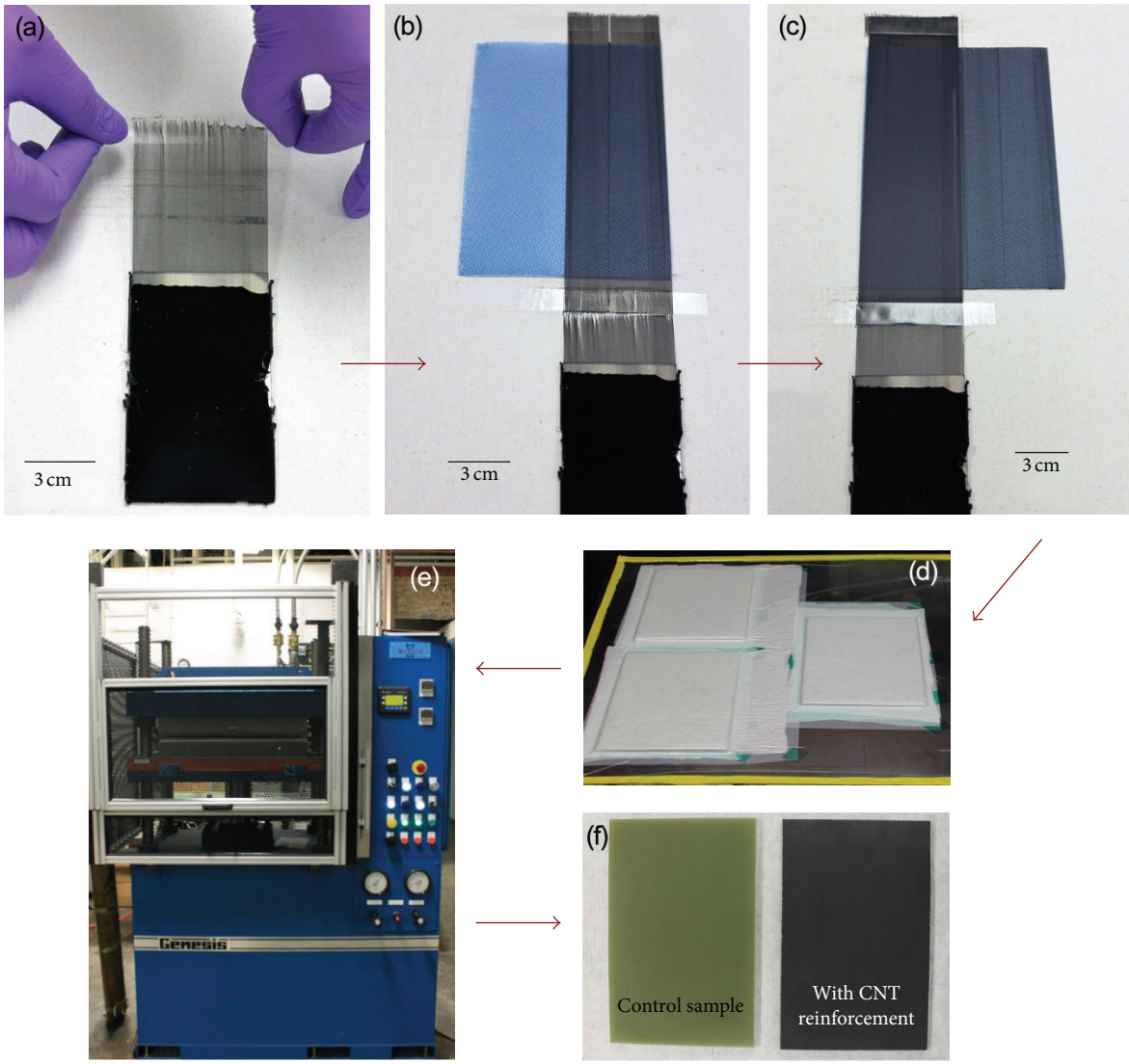

Figure 1: Fabrication of composites with CNT sheet interlayers. (a–c) Drawing 50 mm wide CNT sheets across the prepreg fabric. The sheets easily adhered to the tacky surface. (d, e) The panels were fabricated using vacuum bagging and hot pressing. (f) Both baseline samples and CNT modified samples were created.

Load and displacement values were noted manually for each marking when the crack propagated through it. After load versus displacement values were generated it was noticed that some loading plots did not intersect with the origin. This result can originate from clamping, zeroing the load incorrectly or slight variation in hinge alignment. However, since the flexural modulus of the hinge is constant, the curves could be adjusted so that the slope of the loading curve intersected with the origin. G_{Ic} values were then calculated using the nonlinearity method and the modified beam theory. Only samples types which gave a positive increase in the G_{Ic} initiation valves were selected for further mechanical testing.

A three-point bending fixture from Test Resources was used to apply forward shear Mode II loading to the specimens at a constant crosshead speed of 0.5 mm/min and load point displacement was collected using an independent extensometer from Epsilon Technology Corporation. A span length of 100 mm was used and the support fixtures had radii of 6 mm. Scanning electron microscopy of Mode I and Mode II specimens was completed to examine the fractured surface from crack initiation and propagation from a = 0 mm-1 mm.

SBS testing was used to measure the short beam strength of the specimens according to a research which suggested modifications to ASTM D2344/D2344M-00 [45] to achieve shear failure [46]. This test involves the loading of the specimen with a 3-point bending fixture in order to induce interlaminar failure along the midplane. A 32-ply symmetric laminate was stacked and consolidated to fabricate SBS specimens. A span to thickness ratio was 6.5 and width to thickness ratio of 1.8 was used for achieving shear failures.

Table 1: Calculated average G_{Ic} initiation values and percent change for DCB samples.

	G_{Ic} (kJ/m^2)	SD	% change
Baseline	0.186	0.037	—
2-layer parallel	0.273	0.058	46.77
2-layer perpendicular	0.225	0.094	20.97
4-layer perpendicular	0.102	0.005	−45.16
8-layer perpendicular	0.097	0.02	−47.85

Span length used for SBS testing was 36 mm. The loading was applied at a constant crosshead speed of 1.5 mm/min.

Tensile properties of the composite specimen were tested according to ASTM D3039/D3039M-08 [47]. A 12-ply symmetric laminate was stacked and consolidated to fabricate tensile specimens. For this test, every interlayer was modified by the CNT sheets. The length of the specimens was 250 mm with a width and thickness of 20 mm and 2.2 mm, respectively. The specimen was tabbed on both the ends with G-10 glass fiber epoxy laminates. A laser extensometer was used to determine the sample strain. A displacement rate of 1 mm/min was used to carry out the tests. Each of the four mechanical characterization techniques had a minimum of six replications per sample type.

An Agilent 34420A Micro Ohm Meter was used to measure the electrical resistance of the CNT modified specimen using four-probe method to minimize contact resistance. Electrical resistance was measured in-plane and through the thickness directions for the 12-ply composite laminate. For this test, every interlayer was modified by the CNT sheets. 50 × 20 mm and 20 × 20 mm specimens were used to calculate the resistivity in the in-plane directions and through thickness direction, respectively. Contact wires were attached to the sample through silver epoxy.

3. Results and Discussion

Figure 2 shows the average R-curves for the DCB specimen. A plateau region was never achieved for any samples; thus it was not possible to assign an average value to G_{Ic} propagation. Therefore only G_{Ic} initiation values are reported in Table 1. Addition of aligned sheets of MWCNTs in between the plies affected the Mode I behavior significantly in both the positive and negative manner. The G_{Ic} initiation value of 4- and 8-layer perpendicular samples seemed to decrease by 45.16% and 47.85%, respectively. An average increase of 46.77% and 20.97% was observed in the G_{Ic} initiation values for 2-layer parallel and perpendicular samples, respectively. Figure 3 shows SEM images of the Mode I fractured surface of representative DCB specimens of all the sample types. For baseline samples, a relatively smooth interfacial surface resulted from fiber-matrix debonding. A thick sheet of resin infused CNT layer is seen on the fracture surface for the 4- and 8-layer perpendicular samples. The 2-layer samples showed CNTs embedded in the resin with CNT ruptures and pullout which are likely the mechanisms that increased the G_{Ic} initiation value.

Table 2: Calculated average G_{IIc} initiation values and percent change for ENF samples.

	G_{IIc} (kJ/m^2)	SD	% change
Baseline	0.467	0.067	—
2-layer parallel	0.438	0.062	−6
2-layers perpendicular	0.547	0.041	17

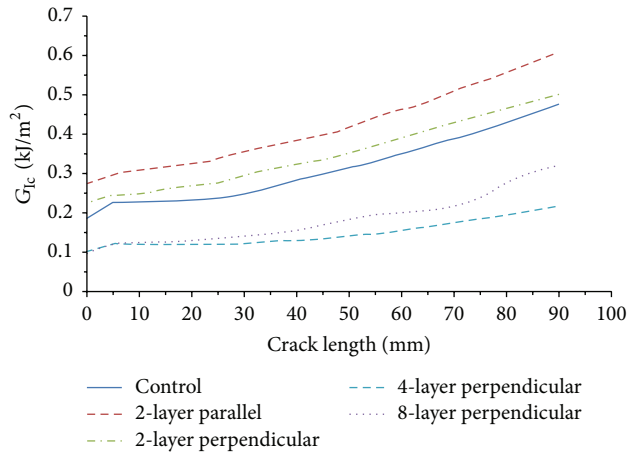

Figure 2: Average G_{Ic} versus crack length curves for baseline samples and CNT sheet interlayer modified samples.

SEM images of 4- and 8-layer perpendicular samples show a layer of pure CNT/epoxy with very few glass fibers from the fabric apparent. Instead of toughening the laminate this highly CNT-reinforced layer of matrix allowed the crack to travel easily through the midplane without any fiber/epoxy debonding or fiber bridging occurring. Because 4-layer and 8-layer samples showed the presence of excess nanotubes in the midplane and significantly decreased the Mode I toughness, the samples were not fabricated for any other tests.

During the ENF flexure text the crack propagation was abrupt which prevented the data collection necessary to calculate G_{IIc} propagation values. Therefore only G_{IIc} initiation values were calculated and reported in Table 2. The calculated average G_{IIc} initiation value for the 2-layer parallel sample was reduced by 6.2% whereas an increase of 17.13% was seen for 2-layer perpendicular sample with respect to the average initiation value of baseline sample.

The mechanism majorly responsible for Mode II fracture behavior is shear yielding of the matrix which results in formation of hackles at the fractured surface. CNT rupture and pull-out are seen in the SEM images of the fracture surface of the ENF samples in Figure 4, but their occurrence with respect to the shear yielded resin hackles is minimal. The number of hackles seen in the SEM image of 2-layer parallel sample is comparable to that seen in the baseline sample, but the size of hackles created in the latter seems to be larger than that of the former. SEM images of 2-layer perpendicular sample generally showed larger and higher number of hackles along with a higher presence of CNT rupture and pull-out, which may provide explanation for the 17.13% increase in

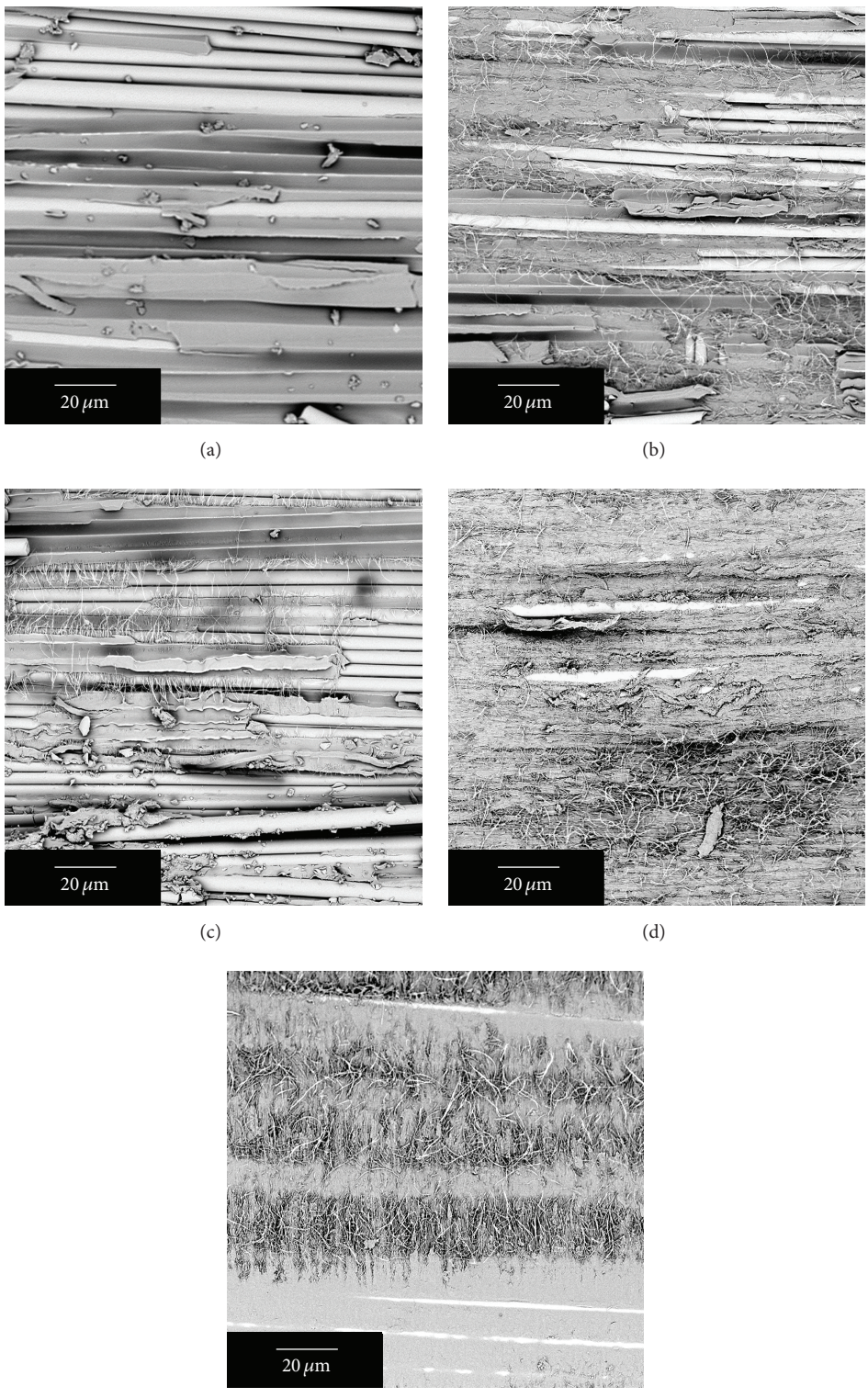

(a) (b) (c) (d) (e)

Figure 3: SEM images taken from the fracture surface of DCB samples, (a) baseline, (b) 2-layer parallel, (c) 2-layer perpendicular, (d) 4-layer perpendicular, and (e) 8-layer perpendicular.

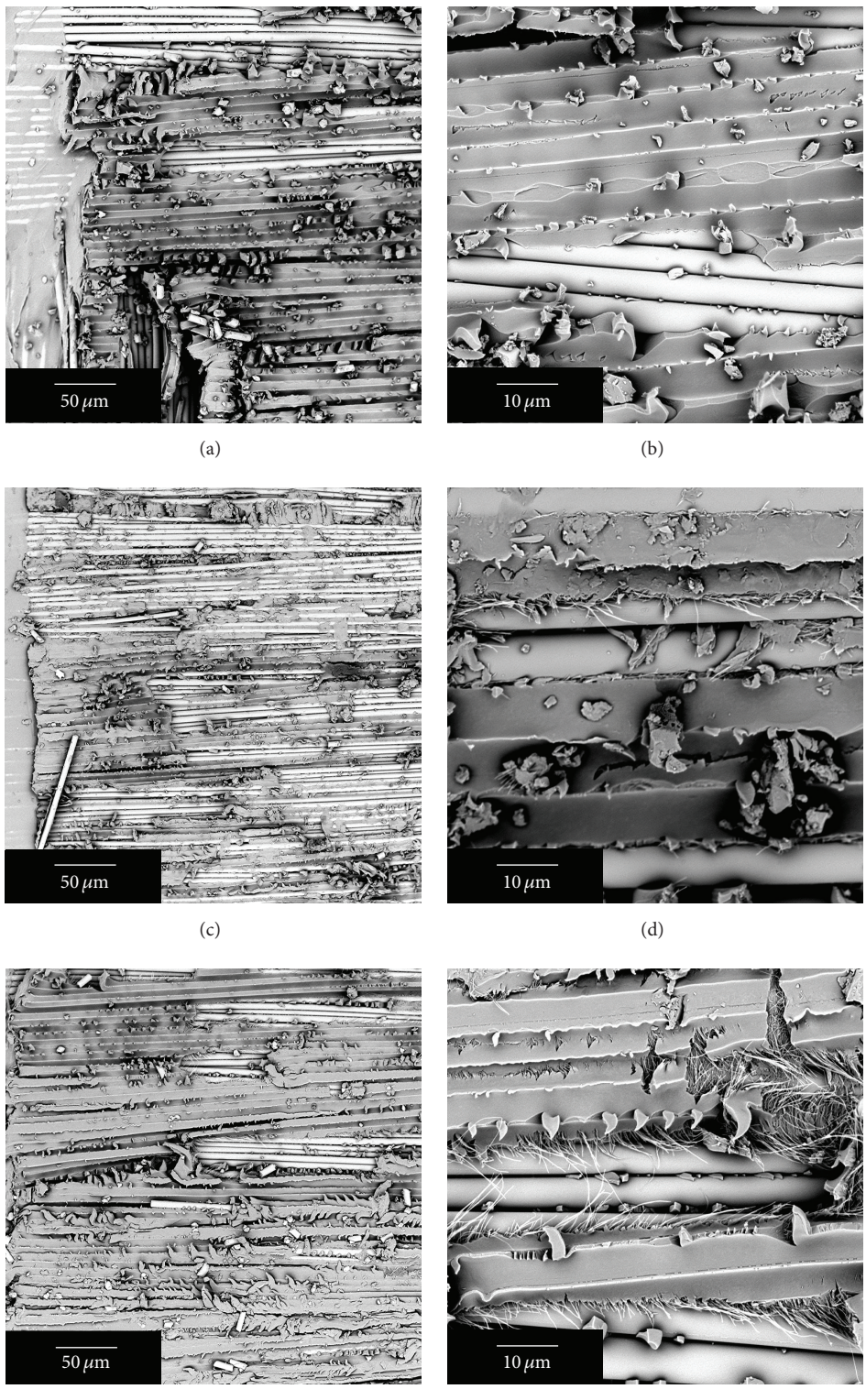

Figure 4: SEM images taken from the fracture surface of ENF samples at two magnifications: (a, b) baseline, (c-d) 2-layer parallel, and (e-f) 2-layer perpendicular.

Table 3: Calculated average short beam strength and tensile properties of baseline and 2-layer CNT sheet modified samples.

	SBS (MPa)	SD	Tensile strength (MPa)	SD	E (GPa)	SD
Baseline	44.9	0.97	557	12.5	23.3	2.16
2-layer parallel	44.1	0.96	557	11.7	23.8	2.19
2-layer perpendicular	44.4	1.12	561	19.8	24.0	2.83

Table 4: Average resistance values measured across the samples and calculated electrical conductivity.

	Electrical resistance (kΩ)	Conductivity (S/m)
2-layer parallel	0.079	14.8
2-layer perpendicular	1.23	0.99
Through thickness	9.68	0.0013

the stress energy release rate of Mode II fracture at crack initiation with respect to that of baseline sample.

The short beam strength results showed similar load versus displacement curves for all the tested sampled. The average values are listed in Table 3. It was observed that the shear failure in the SBS specimens did not occur typically at exactly the specimen midplane; however the failure still occurred within the CNT modified section of the SBS samples.

Tensile testing provided very similar results to the SBS testing. Very similar stress versus strain curves were observed for all the specimens. Table 3 shows the average ultimate tensile strength and modulus value of every tested specimen. No significant change in the magnitude of either property was seen for the CNT modified samples over the baseline sample. Here we can conclude that the in-plane properties were not compromised. It was not surprising that we did not see a significant increase in the in-plane properties because the overall fraction of the CNTs in the sample was very small.

Table 4 shows the electrical resistivity data for the CNT modified composites in the in-plane and through thickness directions. Electrical conductivity achieved in our samples by using just 0.1 wt% aligned carbon nanotube sheet was higher when compared to that achieved by using other forms of CNT reinforced in traditional composites at similar weight fractions of CNTs [26, 33–35]. The conductivity of the perpendicular aligned CNT sheet modified specimen was 15 times lower than that of the parallel aligned CNT sheet modified composites. This is attributed to the anisotropic nature of the CNT sheets themselves. Resistivity values measured in the through thickness (out-of-plane) direction were surprising. It was expected that the very long CNTs would prevent their migration around fibers and through the thickness of the composite, resulting in no measureable electrical conductivity. However, the sample did show conductivity through the thickness of the samples meaning that some CNTs were able to migrate around the fibers in the woven fabric and make contact with others on the next layer. This helps to further explain why an increase in the mode I fracture toughness was achieved.

4. Conclusions

MWCNT sheets were drawn from large CNT arrays and placed onto the sticky surface of woven glass prepregs. Uniform CNT sheet placement throughout the laminate was achieved with active control over CNT location and orientation due to the anisotropic alignment of CNTs within the sheets. Use of optimized number of CNT sheet layers provided an improvement in the initiation interlaminar fracture toughness, which is one of the most significant limitations of 2D composite laminates. The in-plane mechanical properties of the CNT modified composite laminates were not compromised in order to improve their through thickness properties. Modifying the composite laminate with aligned CNT sheets imparted in-plane and the through thickness electrical properties to the initially nonconductive glass-epoxy composite laminate. The improvement in the through thickness properties achieved, for samples with two CNT sheet layers, was attributed to the mechanisms of CNT crack bridging, fracture, and pull-out.

Conflict of Interests

The authors declare that there is no conflict of interests regarding the publication of this paper.

Acknowledgment

This work was partially funded by the Air Force Office of Scientific Research Grant no. FA9550-12-1-0170.

References

[1] A. T. Seyhan, M. Tanoglu, and K. Schulte, "Mode I and mode II fracture toughness of E-glass non-crimp fabric/carbon nanotube (CNT) modified polymer based composites," *Engineering Fracture Mechanics*, vol. 75, no. 18, pp. 5151–5162, 2008.

[2] M. Tanoglu and A. T. Seyhan, "Investigating the effects of a polyester preforming binder on the mechanical and ballistic performance of E-glass fiber reinforced polyester composites," *International Journal of Adhesion and Adhesives*, vol. 23, no. 1, pp. 1–8, 2003.

[3] J. Zhu, A. Imam, R. Crane, K. Lozano, V. N. Khabashesku, and E. V. Barrera, "Processing a glass fiber reinforced vinyl ester composite with nanotube enhancement of interlaminar shear strength," *Composites Science and Technology*, vol. 67, no. 7-8, pp. 1509–1517, 2007.

[4] V. Álvarez, C. R. Bernal, P. M. Frontini, and A. Vázquez, "The influence of matrix chemical structure on the mode I and II interlaminar fracture toughness of glass-fiber/epoxy composites," *Polymer Composites*, vol. 24, no. 1, pp. 140–148, 2003.

[5] A. C. Garg, "Delamination—a damage mode in composite structures," *Engineering Fracture Mechanics*, vol. 29, no. 5, pp. 557–584, 1988.

[6] N. Sela and O. Ishai, "Interlaminar fracture toughness and toughening of laminated composite materials: a review," *Composites*, vol. 20, no. 5, pp. 423–435, 1989.

[7] E. Wu and J. Liau, "Impact of unstitched and stitched laminates by line loading," *Journal of Composite Materials*, vol. 28, no. 17, pp. 1640–1658, 1994.

[8] A. P. Mouritz, "Review of z-pinned composite laminates," *Composites Part A: Applied Science and Manufacturing*, vol. 38, no. 12, pp. 2383–2397, 2007.

[9] A. P. Mouritz, C. Baini, and I. Herszberg, "Mode I interlaminar fracture toughness properties of advanced textile fibreglass composites," *Composites Part A: Applied Science and Manufacturing*, vol. 30, no. 7, pp. 859–870, 1999.

[10] V. A. Guénon, T.-W. Chou, and J. W. Gillespie Jr., "Toughness properties of a three dimensional carbon-epoxy composite," *Journal of Materials Science*, vol. 24, no. 11, pp. 4168–4175, 1989.

[11] W. J. Gilwee and Z. Nir, "Toughened reinforced epoxy composites with brominated polymeric additives," US Patent 6-493865, 1983.

[12] S. U. Khan and J.-K. Kim, "Improved interlaminar shear properties of multiscale carbon fiber composites with bucky paper interleaves made from carbon nanofibers," *Carbon*, vol. 50, no. 14, pp. 5265–5277, 2012.

[13] R. E. Evans and J. E. Masters, "A new generation of epoxy composites for primary structural applications," in *ASTM Toughened Composite Symposium*, Houston, Tex, USA, March 1985.

[14] R. J. Sager, P. J. Klein, D. C. Davis, D. C. Lagoudas, G. L. Warren, and H.-J. Sue, "Interlaminar fracture toughness of woven fabric composite laminates with carbon nanotube/epoxy interleaf films," *Journal of Applied Polymer Science*, vol. 121, no. 4, pp. 2394–2405, 2011.

[15] D. Stevanovic, S. Kalyanasundaram, A. Lowe, and P.-Y. B. Jar, "Mode I and mode II delamination properties of glass/vinylester composite toughened by particulate modified interlayers," *Composites Science and Technology*, vol. 63, no. 13, pp. 1949–1964, 2003.

[16] E. Bozkurt, E. Kaya, and M. Tanoglu, "Mechanical and thermal behavior of non-crimp glass fiber reinforced layered clay/epoxy nanocomposites," *Composites Science and Technology*, vol. 67, no. 15-16, pp. 3394–3403, 2007.

[17] K. V. Arun, S. Basavarajappa, C. Chandrakumar, and S. M. Yadav, "Influence of secondary fillers on the behavior of translaminar failure in glass-epoxy composites," *Polymer—Plastics Technology and Engineering*, vol. 49, no. 5, pp. 495–502, 2010.

[18] A. Warrier, A. Godara, O. Rochez et al., "The effect of adding carbon nanotubes to glass/epoxy composites in the fibre sizing and/or the matrix," *Composites—Part A: Applied Science and Manufacturing*, vol. 41, no. 4, pp. 532–538, 2010.

[19] L. Gorbatikh, S. V. Lomov, and I. Verpoest, "Nano-engineered composites: a multiscale approach for adding toughness to fibre reinforced composites," *Procedia Engineering*, vol. 10, pp. 3252–3258, 2011.

[20] S. S. Wicks, R. G. de Villoria, and B. L. Wardle, "Interlaminar and intralaminar reinforcement of composite laminates with aligned carbon nanotubes," *Composites Science and Technology*, vol. 70, no. 1, pp. 20–28, 2010.

[21] C. S. Grimmer and C. K. H. Dharan, "High-cycle fatigue of hybrid carbon nanotube/glass fiber/polymer composites," *Journal of Materials Science*, vol. 43, no. 13, pp. 4487–4492, 2008.

[22] C. S. Grimmer and C. K. H. Dharan, "Enhancement of delamination fatigue resistance in carbon nanotube reinforced glass fiber/polymer composites," *Composites Science and Technology*, vol. 70, no. 6, pp. 901–908, 2010.

[23] E. J. Garcia, B. L. Wardle, A. J. Hart, and N. Yamamoto, "Fabrication and multifunctional properties of a hybrid laminate with aligned carbon nanotubes grown In Situ," *Composites Science and Technology*, vol. 68, no. 9, pp. 2034–2041, 2008.

[24] Z. Shen, S. Bateman, D. Y. Wu, P. McMahon, M. Dell'Olio, and J. Gotama, "The effects of carbon nanotubes on mechanical and thermal properties of woven glass fibre reinforced polyamide-6 nanocomposites," *Composites Science and Technology*, vol. 69, no. 2, pp. 239–244, 2009.

[25] L. Böger, J. Sumfleth, H. Hedemann, and K. Schulte, "Improvement of fatigue life by incorporation of nanoparticles in glass fibre reinforced epoxy," *Composites Part A: Applied Science and Manufacturing*, vol. 41, no. 10, pp. 1419–1424, 2010.

[26] M. H. G. Wichmann, J. Sumfleth, F. H. Gojny, M. Quaresimin, B. Fiedler, and K. Schulte, "Glass-fibre-reinforced composites with enhanced mechanical and electrical properties—benefits and limitations of a nanoparticle modified matrix," *Engineering Fracture Mechanics*, vol. 73, no. 16, pp. 2346–2359, 2006.

[27] J. Kong, N. R. Franklin, C. Zhou et al., "Nanotube molecular wires as chemical sensors," *Science*, vol. 287, no. 5453, pp. 622–625, 2000.

[28] C. Dekker, "Carbon nanotubes as molecular quantum wires," *Physics Today*, vol. 52, no. 5, pp. 22–28, 1999.

[29] S. Peng, J. O'Keeffe, C. Wei et al., "Carbon nanotube chemical and mechanical sensors," in *Proceedings of the 3rd International Workshop on Structural Health Monitoring*, pp. 1–8, Stanford, Calif, USA, 2001.

[30] E. T. Thostenson and T.-W. Chou, "Carbon nanotube networks: sensing of distributed strain and damage for life prediction and self healing," *Advanced Materials*, vol. 18, no. 21, pp. 2837–2841, 2006.

[31] F. H. Gojny and K. Schulte, "Functionalization effect on thermomechanical behavior of multiwalled carbon nanotube/epoxy composites," *Composites Science and Technology*, vol. 34, pp. 2303–2308, 2004.

[32] F. H. Gojny, M. H. G. Wichmann, U. Köpke, B. Fiedler, and K. Schulte, "Carbon nanotube-reinforced epoxy-composites: enhanced stiffness and fracture toughness at low nanotube content," *Composites Science and Technology*, vol. 64, no. 15, pp. 2363–2371, 2004.

[33] F. H. Gojny, M. H. G. Wichmann, B. Fiedler, W. Bauhofer, and K. Schulte, "Influence of nano-modification on the mechanical and electrical properties of conventional fibre-reinforced composites," *Composites—Part A: Applied Science and Manufacturing*, vol. 36, no. 11, pp. 1525–1535, 2005.

[34] S.-M. Yuen, M. Chen-Chi, H.-H. Wu et al., "Preparation and thermal, electrical, and morphological properties of multiwalled carbon nanotube and epoxy composites," *Journal of Applied Polymer Science*, vol. 103, no. 2, pp. 1272–1278, 2007.

[35] Z. Spitalsky, D. Tasis, K. Papagelis, and C. Galiotis, "Carbon nanotube-polymer composites: chemistry, processing, mechanical and electrical properties," *Progress in Polymer Science*, vol. 35, no. 3, pp. 357–401, 2010.

[36] A. Moisala, Q. Li, I. A. Kinloch, and A. H. Windle, "Thermal and electrical conductivity of single- and multi-walled carbon nanotube-epoxy composites," *Composites Science and Technology*, vol. 66, no. 10, pp. 1285–1288, 2006.

[37] A. T. Seyhan, F. H. Gojny, M. Tanoglu, and K. Schulte, "Critical aspects related to processing of carbon nanotube/unsaturated thermoset polyester nanocomposites," *European Polymer Journal*, vol. 43, no. 2, pp. 374–379, 2007.

[38] S. C. Joshi and V. Dikshit, "Enhancing interlaminar fracture characteristics of woven CFRP prepreg composites through CNT dispersion," *Journal of Composite Materials*, vol. 46, no. 6, pp. 665–675, 2012.

[39] V. P. Veedu, A. Cao, X. Li et al., "Multifunctional composites using reinforced laminae with carbon-nanotube forests," *Nature Materials*, vol. 5, no. 6, pp. 457–462, 2006.

[40] Y. Inoue, K. Kakihata, Y. Hirono, T. Horie, A. Ishida, and H. Mimura, "One-step grown aligned bulk carbon nanotubes by chloride mediated chemical vapor deposition," *Applied Physics Letters*, vol. 92, no. 21, Article ID 213113, 2008.

[41] K. Fu, O. Yildiz, H. Bhanushali et al., "Aligned carbon nanotube-silicon sheets: a novel nano-architecture for flexible lithium ion battery electrodes," *Advanced Materials*, vol. 25, no. 36, pp. 5109–5114, 2013.

[42] M. Kotaki and H. Hamada, "Effect of interfacial properties and weave structure on mode I interlaminar fracture behavior of glass satin woven fabric composites," *Composites Part A: Applied Science and Manufacturing*, vol. 28, no. 3, pp. 257–266, 1997.

[43] ASTM, "Standard test method for mode I interlaminar fracture toughness of unidirectional fiber-reinforced polymer matrix composites," ASTM Standard D5528-01, American Society for Testing and Materials, West Conshohocken, Pa, USA, 2007.

[44] K. Jis, *Testing Methods for Interlaminar Fracture Toughness of Carbon Fibre Reinforced Plastics*, Japanese Standards Association, Tokyo, Japan, 1993.

[45] ASTM Standard D 2344/D 2344M–00, *Standard Test Method for Short-Beam Strength of Polymer Matrix Composite Materials and Their Laminates*, American Society for Testing and Materials, West Conshohocken, Pa, USA, 2006.

[46] D. F. Adams and J. M. Busse, "Suggested modifications of the short beam shear test method," in *Proceedings of the 49th International SAMPE Symposium and Exhibition: Materials and Processing Technology*, pp. 1–14, Long Beach, Calif, USA, May 2004.

[47] ASTM Standard D3039/D3039M-08, *Standard Test Method for Tensile Properties of Polymer Matrix Composite Materials*, American Society for Testing and Materials, West Conshohocken, Pa, USA, 2008.